Chapter 4

Introduction

Metal complexes of synthetic porphyrins have been used as catalysts for the oxygenation of organic substrates for more than 20 years. The most intensively investigated complexes are with Cr, Mn, and Fe, all of which form reactive metal-oxo species (Mn ≥ Fe >> Cr). [1-6] In some limited cases the biological conditions under which cytochrome P-450 operates, O_2 and reductant, could be mimicked.[7] Still, most of the work was driven toward what might be viewed as peroxidase mimics, i.e., the use of exogenic oxidants (similar to H_2O_2 in biological systems).[8-10] The Holy Grail in homogeneous oxidation catalysis, transferring the oxygen atom(s) of O_2 into substrates without any other additives (neither reductant nor oxidant), has not been realized so far with first-row transition metals although perhalogenated iron porphyrins have been used for the aerobic autooxidation of hydrocarbons.[11-14] The only example up to now remains the Quinns-Groves system that relies on dioxoruthenium(VI) as oxidant and on the disproportionation of oxoruthenium(IV) to dioxoruthenium(VI) and the dioxygen-activating ruthenium(II). One main limitation of this system is product-inhibition: the reactivity of the ruthenium(II) intermediate is gradually reduced during the process due to coordination of the epoxide. [15,16]

Increasing attention is given in recent years to porphyrin-like macrocycles with the aim of modifying the intrinsic properties of porphyrins as to fit special needs. This is also true for catalysis, in which corroles play a major role. The potential of metal corroles as catalysts is gradually been revealed, mainly with the iron, manganese, and rhodium complexes of $(tpfc)H_3$ (**1**, see Scheme 4.1 for all the complexes discussed later). [17,18] Metal-oxo species have been obtained so far with manganese(V) (spectroscopy) and chromium(V) **(2)** (spectroscopy and X-ray crystallography). In a most recent report we have demonstrated that chromium corroles can be isolated in four oxidation states, and most importantly, that the chromium(III) complexes **3** and **5** react with O_2 to form (oxo)chromium(V) (**2**). [19]

Scheme 4.1. Numbering scheme for the various chromium compounds.

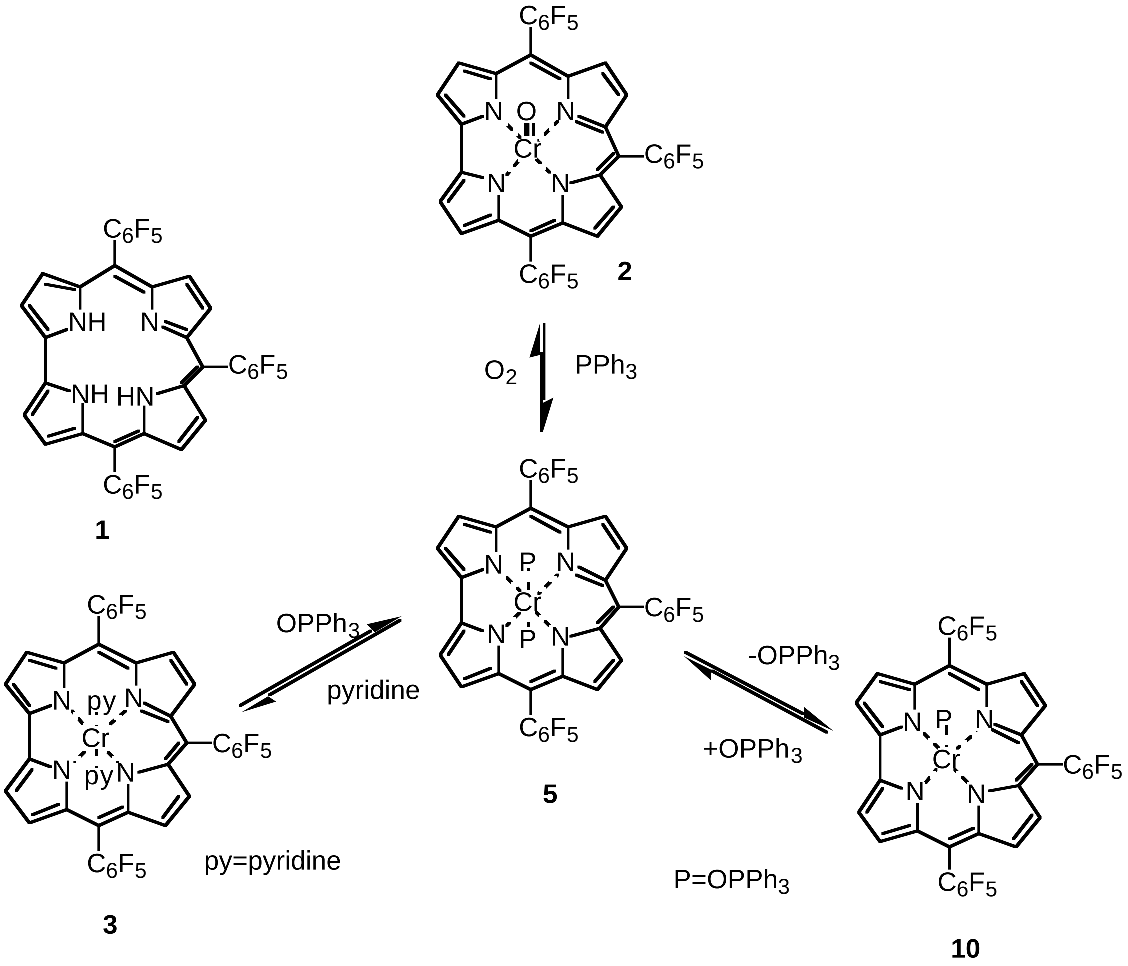

1
2
O2
PPh3
5
OPPh3
pyridine
3
py=pyridine
-OPPh3
+OPPh3
10
P=OPPh3
C6F5
N
NH
HN
Cr
O
P
py

The last observation opens up the possibility that the $Cr^{V}O/Cr^{III}$ cycle could be used to activate molecular oxygen towards transfer to a substrate. Mechanistic information about the various processes was obtained by kinetic experiments.

Experimental Section

Methods

Spectroscopy

EPR spectra were obtained on a Bruker EMX ER 082 spectrometer equipped with a liquid helium cryostat (Oxford) for low temperature measurements. UV-Vis spectra were measured on a HP 8452 spectrophotometer. GC-MS was performed on a HP gas chromatograph with a HP-1 column (length: 30m) using EI-MS as a detector. Calibration samples for GC were made by adding 100 µL of styrene and 100 mg iodosylbenzene to 1 mL of a dilute solution of (tetrakis-perfluorophenylporphyrinato)iron(III) chloride in $CDCl_3$. After the oxidant was consumed (the solution became clear), composition was determined by ^{1}H-NMR and used to calibrate the observed GC traces.

Electrochemistry

Voltametric measurements were made on a CHI660 workstation with a normal three-electrode configuration, consisting of a glassy carbon electrode, an Ag/AgCl reference electrode, and a Pt-wire auxiliary electrode. Samples were in the milimolar range in 0.1 M $[Bu_4N]PF_6/CH_2Cl_2$ solution at room temperature.

Materials

All chemicals were purchased either from Aldrich or EM Science (solvents) and mostly used as received. $OPPh_3$ and PPh_3 were recrystallized before use, the olefins were passed through a small column of basic alumina just prior to use, and tetrabutylammonium hexafluorophosphate was recrystallized from ethanol/ether.

Kinetic measurements

Oxidation of PPh_3 by (tpfc)Cr(O) (2)

Accurate amounts (in the range of 400-800 μL) from an 8.75 mM PPh_3/toluene solution were added under argon to a stock solution of **2** in toluene and the total volume was adjusted to 2 mL. The time-dependent absorbances at 464 nm (product) and 404 nm (reagent) were monitored at 25 ˚C and used for data analysis.

Aerobic oxidation of 5 to 2

a) determination of the order in **5**: A stock solution was prepared by dissolving about 2 mg **2** and 1 mg PPh_3 in about 2 mL methylene chloride under argon. A 2 mL solution of 1.124 mM $OPPh_3/CH_2Cl_2$ was put in a cuvette, and 50 μL from the stock solution was added via syringe. The observed trace of the time-dependent change at 466 nm was used to determine half-lives at different points in the reaction, from which the order in **5** was computed. b) as a function of the concentration of O_2: A cuvette, equipped with a high-vacuum teflon stopcock and connected via a side-arm to a 10-mL round-bottom flask, was evacuated and refilled with argon three times. 4 mL of a degassed and argon purged methylene chloride solution (0.6 mM $OPPh_3$ and approximatively 10 μM of **5**) were transferred into the cuvette via canula. The apparatus was evacuated and the solvent transferred to the side arm via vacuum transfer, leaving the solid residues behind. The required pressure of O_2 was introduced while frozen and the thawed solvent was left to equilibrate for 30 min. The oxygenated solvent was then transferred back in the cuvette by tipping the apparatus. The changes in the absorbance were followed at 466 nm for the following partial pressures of O_2: 108, 208, 308, and 408 mmHg. c) as a function of the concentration of $OPPh_3$: 2 mL of a solution were placed into a cuvette and 50 μL from a stock solution of the complex (2 mg **2** and 1 mg PPh_3 in 2 mL toluene under argon) was added. The changes in the absorbance at 466 nm versus time were monitored, repeating the process with various concentrations of $OPPh_3$ (in the range 0.2-0.8 mM). d) Independent measurement of axial ligand dissociation: A stock solution was prepared by dissolving 16 mg **2** with 4 mg each $OPPh_3$ and PPh_3 in 5 mL degassed methylene chloride under argon. A cuvette and its side-arm flask (see b) for description) were filled with degassed methylene chloride, and a few drops of the stock solution were added to the cuvette. The initial spectrum was measured. The content of the cuvette was diluted by adding solvent from the side-arm flask, and a spectrum was taken after each dilution. After the last spectrum was taken, a small amount of solid $OPPh_3$ was added to the content of the cuvette and the spectrum of the non-dissociated complex was obtained. From this, the isosbestic point could be measured and the dilution of each sample calculated, assuming a constant isosbestic point. The data were fit as described in the

Results section.

Results

Kinetic analysis for oxygenation of 5 to 2

The spectral changes upon exposure to air of a CH_2Cl_2 solution of **5** and excess $OPPh_3$ are shown in Figure 4.1. Clearly, the isosbestic points indicate that here is no appreciable accumulation of any intermediate in the transformation of **5** to **2**. In order to learn more about the details of this multistep reaction, the reaction order in all the components was examined as follows:

a) Reaction order in chromium: Although the kinetic traces (see Figure 4.1 (insert) for an example) looked like a first order decay, this was confirmed by examining the changes of half-life times during the course of reaction and applying the following equation:

$$\begin{aligned} rate &= k[\mathbf{5}]^n \\ \ln(t_{1/2}) &= (1-n)\ln([\mathbf{5}]) - \ln(k) \end{aligned} \qquad (1)$$

where $t_{1/2}$ is the time required for any [**5**] to decay to [**5**]/2. The absorbance is related to the concentration by:

$$\frac{OD - OD_\infty}{OD_0 - OD_\infty} = \frac{[\mathbf{5}]}{[\mathbf{5}]_0} \qquad (2)$$

where OD, OD_0., and OD_∞ are the observed absorbance at any time, at time zero, and at infinite time, respectively. Combining both equations results in:

$$\ln(t_{1/2}) = (1-n)\ln(OD - OD_\infty) + cste \qquad (3)$$

For the trace shown in Figure 4.3, $t_{1/2}$ was measured for the first 4 half times. Using the above equation) results in: n=1.09 for 3 $t_{1/2}$'s, and n=1.2 for 4 $t_{1/2}$'s. This clearly indicates that the reaction is first order in chromium.

b) Reaction order in O_2: Four measurements were performed, wherein the amount of $OPPh_3$ (0.60 mM) and **5** (about 10 μM) were kept constant, while the partial pressure of oxygen above the solution was varied. Assuming the validity of Henry's law, the concentration of oxygen in solution is directly proportional to its partial pressure. In any case, the concentration of dissolved oxygen is high enough relative to **5** as to assure its pseudo first order decay. The general equation that applies is

$$\begin{gathered} \ln(k_{obs}) = \ln(k) + n\ln(pO_2) \\ n: \quad order \quad in \quad O_2 \end{gathered} \tag{4}$$

and n was found to be 1.05. This is further exemplified by the linear plot in Figure 4.2, i.e., the reaction is first order in O_2.

c) Reaction order in $OPPh_3$: The response of the rate constant to variations in the concentration of $OPPh_3$ (large excess relative to **5**) in toluene solutions at fixed concentrations of **5** and O_2 is clearly inverse, but not linear (Figure 4.3). This really suggests that ligand dissociation is a fast pre-equilibrium step for the rate limiting reaction of the penta-coordinated complex **10** with O_2 (Scheme 4.2 and Equation 5). To account for this, we propose that the hexa-coordinate **5** does not react directly with oxygen. A ligand dissociation step has to take place first, i.e. only the penta-coordinated species is reactive

Figure 4.1. Spectral changes upon aerobic oxidation of a 12.8 μM solution of **5** in 1.69 mM $OPPh_3/CH_2Cl_2$.

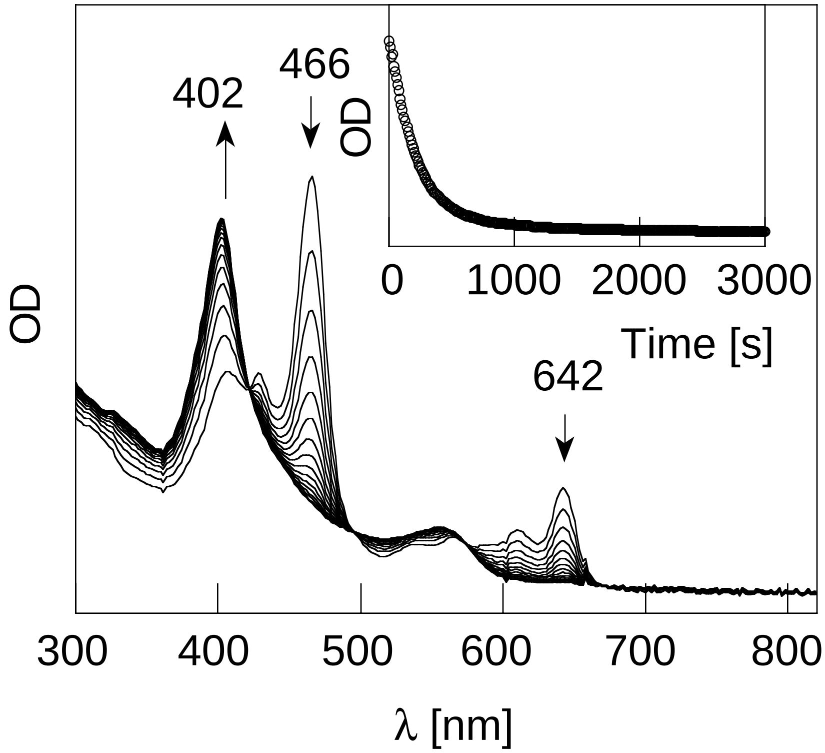
402
466
642
OD
300
400
500
600
700
800
λ [nm]
OD
0
1000
2000
3000
Time [s]

Figure 4.2. Plot of k_{obs} as a function of the partial pressure of oxygen, for the transformation of **5** to **2**.

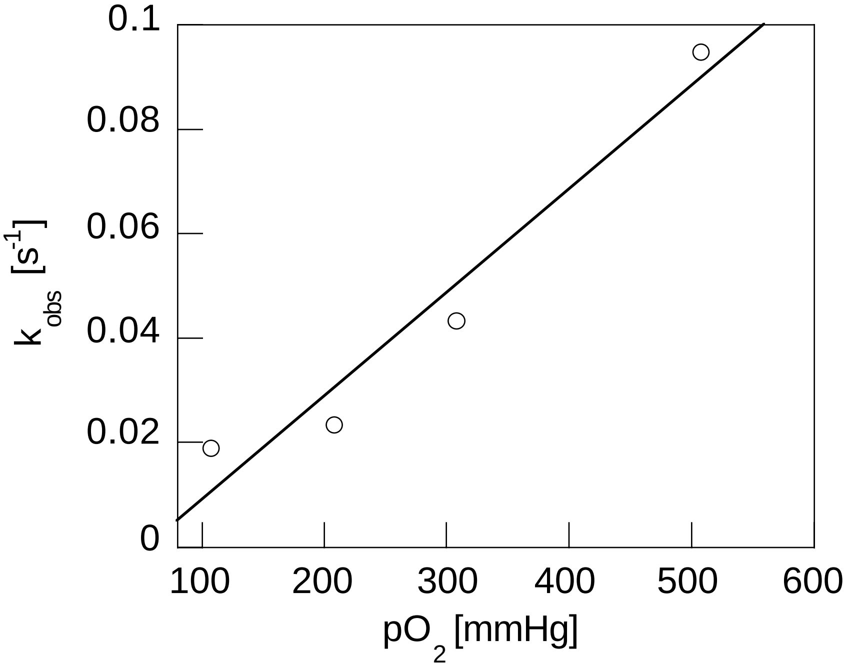
0.1
0.08
0.06
0.04
0.02
0
k_{obs} [s^{-1}]
100
200
300
400
500
600
pO_2 [mmHg]

towards O_2. Having confirmed already the first order dependence on **5** and O_2 readily enforces the conclusion that reaction of (tpfc)Cr^{III}($OPPh_3$) with O_2 is rate limiting, i.e:

Scheme 4.2

$$\mathbf{5}\xrightleftharpoons{K_1}(tpfc)Cr^{III}(OPPh_3)(\mathbf{10})+OPPh_3$$

$$\mathbf{10}+O_2\xrightarrow{k_2}\quad\rightarrow\quad\rightarrow\mathbf{2}$$

$$\frac{d[\mathbf{2}]}{dt}=k_{obs}[\mathbf{10}][O_2] \qquad (5)$$

Using the classical steady-state approximation for **10**, results in Equation 6, which predicts the inverse order of $OPPh_3$ as well as the linearity with respect to O_2.

$$\frac{d[\mathbf{2}]}{dt}=\frac{k_2K_1}{([OPPh_3])}[\mathbf{5}]\,[O_2] \qquad (6)$$

originating from the reactions depicted in Scheme 4.2. Note that Equation 6 is typical for reactions where an equilibrium step precedes the main reaction.

Accordingly, the measured rate constant (k_{obs}) is indeed expected to be affected by the concentration of $OPPh_3$ in a non-linear fashion:

$$k_{obs}=\frac{k_2K_1}{([OPPh_3])} \qquad (7)$$

A non linear regression of the data presented in Figure 4.3 reveals $k_2K_1=9.624\bullet10^{-8}$ Ms^{-1}

d) Independent measurement of K_1:

By dilution of a solution of **5** under argon, in the absence of any added ligands, the dissociation constant can be measured directly by following changes in the electronic spectrum at 466 nm. The following equation holds for a simple dissociation:

$$\frac{[\mathbf{5}]_0}{\Delta OD} = \frac{\Delta OD}{K\Delta\varepsilon^2} + \frac{1}{\Delta\varepsilon} \qquad (8)$$

where $[\mathbf{5}]_0$ is the concentration of **5** without any dissociation taking place, and ΔOD

Figure 4.3. The rate constants for aerobic oxidation of **5** in CH_2Cl_2 as a function of the concentration of $OPPh_3$.

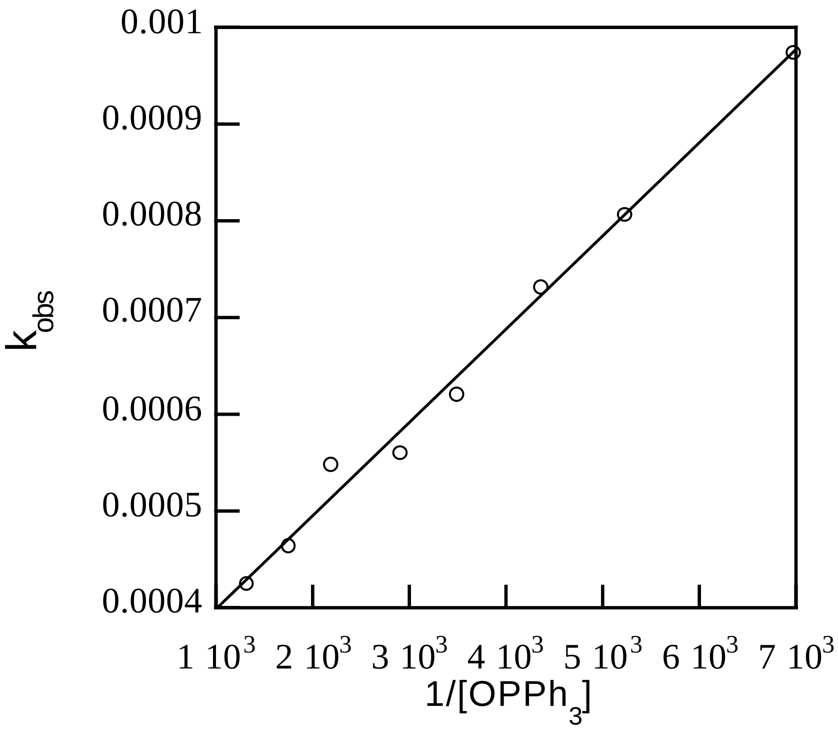
0.001
0.0009
0.0008
0.0007
0.0006
0.0005
0.0004
k_{obs}
$1\ 10^3$
$2\ 10^3$
$3\ 10^3$
$4\ 10^3$
$5\ 10^3$
$6\ 10^3$
$7\ 10^3$
$1/[OPPh_3]$

is the difference OD-OD_0, where OD_0 is the absorbance that would have been observed in the absence of dissociation. Using Equation 8, we found $K_1 = 4.5 \bullet 10^{-5}$ M, which gives the following value for k_2 $2.14 \bullet 10^{-3}$ s^{-1}

Kinetics of oxygen-atom transfer from 2 to PPh_3

The spectroscopic changes upon addition of a large excess of PPh_3 to a solution of **2** (~ 10 μM) in toluene are shown in Figure 4.4 for $[PPh_3]$= 1.82 mM.

A plot of k_{obs} versus the concentration of triphenyl phosphine is linear, as expected for a bimolecular reaction under pseudo first order condition. The second-order rate constant was elucidated as $k = 9.7\ M^{-1}s^{-1}$.

Discussion

The main goals of this work were to elucidate the reaction mechanism of the oxygenation of the chromium(III) corrole (**5**) to the oxochromium complex **2**; to determine the rate constant of the elementary steps involved in the above multi-step reaction; and to determine the reactivity of oxygen atom transfer from **2** to oxophilic substrates.

The kinetic data for the transformation of **5** into **2** in aerobic solutions was found to be first order in O_2 and in Cr^{III}, and inversely correlated to the concentration of $OPPh_3$. This fits perfectly the scenario depicted in Scheme 4.2 dissociation of one $OPPh_3$ ligand from **5** as to form **10**, which reacts with O_2 in a rate limiting step. Interestingly, the kinetic data also fits another scenario, the rate-limiting reaction of **10**-O_2 with another molecule of **10**.

Non-linear regression of the data from the ligand-effect on k_{obs} yielded the composite elementary rate/equilibrium constant k_2/K_1. Separation of the elementary rate and equilibrium constant can and was achieved via an independent measurement of K_1. This was achieved by anaerobic measurements of the dissociation constants of $OPPh_3$ from **5**. The small value of K_1 implies that the complex is never fully dissociated, except in very dilute solutions. The air-sensitivity is mainly due to a very reactive five-coordinate species. Dissociation serves to modulate the reactivity by controlling the amount of reactive species available. Owing to its increased basicity, pyridine would be expected to be a better ligand and lead to a more air-stable Cr^{III} owing to the lower dissociation constant. As we have previously shown, the bis-pyridine complex is ideal for the isolation of chromium corroles in their Cr^{III} oxidation state.

Table 4.2. Kinetic parameters for aerobic oxidation of **5**.

k_2K_1	$9.624 \cdot 10^{-8}$ Ms^{-1}
K_1	$4.5 \pm 2.3 \cdot 10^{-5}$ M
k_2	$2.14 \cdot 10^{-3}$ s^{-1}

Figure 4.4. Spectral changes for the reaction between **2** and PPh_3.

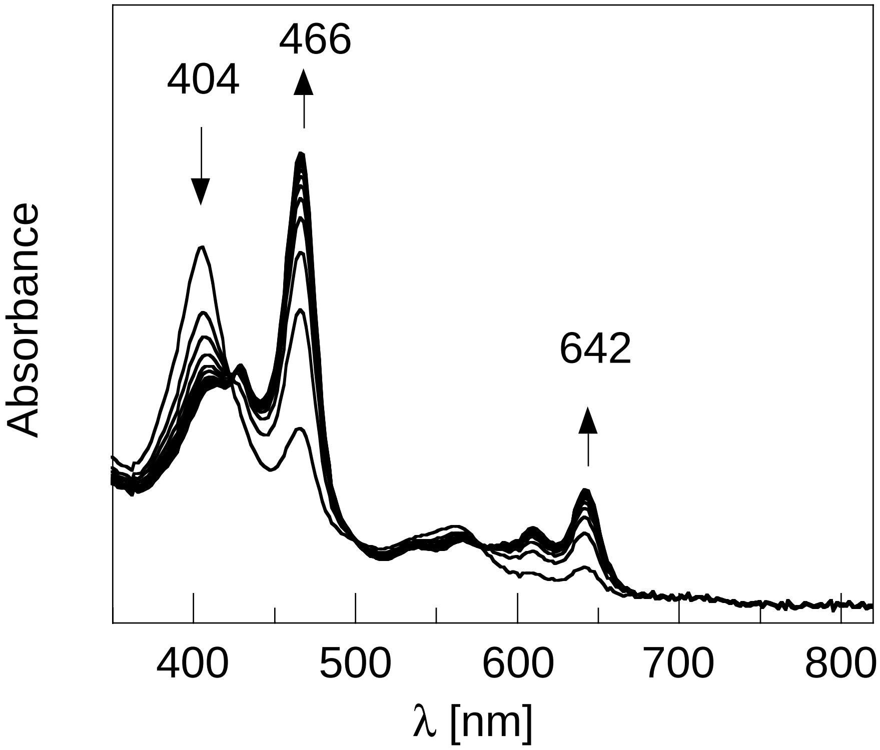
404
466
642
Absorbance
400
500
600
700
800
λ [nm]

The oxo complex **2** reacts with PPh_3 in pseudo-first-order fashion. The reaction is by no means fast, which again underscores the stability of this species. We turned to bromination of the corrole as a means to increase reactivity (see Chapters 5 and 6). Such a strategy has been successfully employed in the case of porphyrins. Even though a perbrominated corrole has been reported in the recent literature, we believe this is the first quantification of the effect of halogenation on corrole metal complex reactivity.

Conclusion

The Cr^{III} oxidation state is quite air-sensitive, contrasting with the normal behavior of this oxidation state. Extensive kinetic analysis has shown the reaction to require ligand dissociation before reaction with O_2. We have extensively characterized the reaction of this species with O_2 to form the corresponding chromium oxo species **2**. While the reaction is quite fast, even at room temperature, the reverse reaction (i.e., oxygen atom transfer) seems to occur only with phosphines as a substrate, and even in that case, the reaction is not as rapid as one would expect. This points to the stability of the metal-oxygen bond in **2** as a major factor in explaining the reactivity of **5**. To move to more interesting substrates, some sort of activation of **2** has to be performed. Since the stability of the high oxidation states is due to the electronegative character of corroles when compared to porphyrins, addition of electronegative substituents might lead to a compound with more desirable properties form a catalytic point of view. This approach will be examined in subsequent chapters.

References

(1) Fuji, H.; Yoshimura, T.; Kamad, H. *Inorg. Chem.* **1997**, *36*, 1122.

(2) Groves, J. T.; Kruper, W. J. *J. Am. Chem. Soc.* **1979**, *101*, 7613.

(3) Groves, J. T.; Haushalter, R. C.; Nakamura, M.; Nemo, T. E.; Evans, B. J. *J. Am. Chem. Soc.* **1981**, *103*, 2884.

(4) Groves, J. T.; Haushalter, R. C. *J. Chem. Soc. , Chem. Commun.* **1981**, 165.

(5) Groves, J. T.; Kruper, W. J.; Haushalter, R. C. *J. Am. Chem. Soc.* **1982**, *104*, 6375.

(6) Hill, C. L.; Schardt, B. C. *J. Am. Chem. Soc.* **1980**, *102*, 6374.

(7) Tabushi, I.; Koga, N. *J. Am. Chem. Soc.* **1979**, *101*.

(8) Oea, S.; Watanabe, Y.; Fujimori, K. *Tetrahedron Lett.* **1982**, *23*, 1189.

(9) Renaud, J. P.; Battioni, P.; Bartoli, J. F.; Mansuy, D. *J. Chem. Soc. , Chem. Commun.* **1983**, 888.

(10) Battioni, P.; Renaud, J. P.; Bartoli, J. F.; Reina-Artiles, M.; Fort, M.; Mansuy, D. *J. Am. Chem. Soc.* **1988**, *110*, 8462.

(11) Ellis, P. E.; Lyons, J. E. *Catal. Lett.* **1989**, *3*, 389.

(12) Ellis, P. E.; Lyons, J. E. *Coor. Chem. Rev.* **1990**, *105*, 181.

(13) Lyons, J. E.; Ellis, P. E. *Catal. Lett.* **1991**, *8*, 45.

(14) Lyons, J. E.; Ellis, P. E.; Myers, H. K.; Wagner, R. W. *J. Catal.* **1993**, *14*, 311.

(15) Groves, J. T.; Quinn, R. *J. Am. Chem. Soc.* **1985**, *107*, 5790.

(16) Groves, J. T.; Quinn, R. *Inorg. Chem.* **1984**, *23*, 3844.

(17) Gross, Z.; Golubkov, G.; Simkhovich, L. *Angew. Chem. , Int. Ed.* **2000**, *39*, 4045.

(18) Simkhovich, L.; Mahammed, A.; Goldberg, I.; Gross, Z. *Chem. Eur. J.* **2001**, *7*, 1041.

(19) Meier-Callahan, A. E.; Di Bilio, A. J.; Simkhovich, L.; Mahammed, A.; Goldberg, I.; Gray, H. B.; Gross, Z. *Inorg. Chem.* **2001**, *40*, 6788.